

THE CHANGES IN STRUCTURE OF STEEL P91 AFTER SHORT ANNEALINGS

KRÁL Lubomír ¹, ČERMÁK Jiří ², KRÁL Petr ¹

^{1,2}*Institute of Physics of Materials, v.v.i., AS CR, ²CEITEC IPM, Brno, Czech Republic, EU*

Abstract

Phase composition of the steel P91 during annealing was studied with the aim to reveal the evolution of new phases. In this paper, the precipitation was characterized using energy-dispersive X-ray spectroscopy (EDS) and electron diffraction in transmission microscopy (TEM). Only Nb-rich particles were found in the studied samples austenitized at 1423 °C for 20h and water cooled. After tempering at 673 °C for 2 h, the formation mainly M₃C type carbides and after tempering at 873 °C for 2 h, the formation of M₇C₃ and M₂₃C₆ was observed. These structure changes play an important role for stability and also carbon diffusion.

Keywords: P91, carbides, carbon, precipitation

1. INTRODUCTION

The Cr-Mo-V steels as P91 are widely used in power and petrochemical plants due to its very well properties as creep resistance, toughness or corrosion at higher temperatures. This high strength steel normally transform completely to martensite during air cooling. The temperature of the martensite start (M_s) is about 673 K, temperature of martensite finish (M_f) is about 473 K [1,2]. Because the content of carbon in this steel is low (up to 0.6 % wt.%), structure of martensite can be described as massive, cubic, lath-like, lenticular, subgrain-containing bundles. Because during undercooling is not possible partitioning, this situation is termed paraequilibrium. In the course of this annealed supersaturated BCC structure becomes unstable and precipitation of secondary phases starts [3].

The precipitation of phases is strongly influenced by the faster diffusing interstitial elements as e.g carbon. The diffusion coefficient of carbon is several orders of magnitude higher than the diffusion coefficients of the substitutional elements. It is clear that the first precipitated phases are carbides. The beginning of the precipitation was studied in work [3]. There no partitioning of Cr, Mo and Mn between cementite and martensite after tempering at 350 °C for 40 h was observed. The content of carbon in carbides was about 10 times higher than content of carbon in the matrix. It was demonstrated, that cementite in Cr and Mo containing alloy steels, precipitates from supersaturated ferrite via paraequilibrium transformation mechanism. The interface concentrations slowly rise from paraequilibrium to equilibrium concentrations.

This precipitation is one of the main factors important for resistance strength under creep condition. The precipitates and also coarsening of secondary phases during heat treatment is crucial point for obtain sufficient structure and mechanical properties. Because this process is strongly connected with diffusion of carbon in supersaturated matrix, it is very useful to clarify this relationship. The carbon diffusion in supersaturated matrix of P91 steel was study in ours work [4]. The most expressive changes of diffusion coefficient of carbon were found in temperature range of 673-873 K. In this paper the changes of structure and carbon diffusion in the steel P91 were studied after short time annealing at temperatures 673 and 873 K.

2. EXPERIMENTAL

In order to dissolving maximum portion of Cr-rich precipitates, the commercial P91 ferrite-martensite chromium steel (0.10 C, 0.40 Mn, 8.5 Cr, 0.10 Ni, 0.88 Mo, 0.23 V, 0.10 Nb, 0.045 N, bal. Fe, all in wt.%) was austenitized at 1423 K for 20 h in pure Ar and then water cooled. The experimental samples (10 mm in

diameter × 4 mm in height) were machined from the annealed ingots. After the pre-annealing, the samples were annealed in a special vacuum furnace ULVAC RIKO MILA-5000 with extremely intensive infrared heating in a vacuum of about 5×10^{-6} mbar at temperatures 673 and 873 K for 2 h. Both the heating and cooling of samples was very rapid (hundreds of Kelvins in the first few seconds at the beginning and the end of the annealing). These samples were labeled as B and C respectively, the austenitized sample as A.

The structure of the samples was analyzed with scanning electron microscope (SEM) Tescan LYRA 3 XMU FEG/SEMxFIB with focused ion beam and energy dispersive spectrometry (EDS) for X-ray microanalysis and using electron backscatter diffraction (EBSD) analysers by Oxford Instruments. The surface of these samples was metallographically grinded and electropolished ($\text{CH}_3\text{COOH} : \text{HClO}_4 = 9 : 1$, 15 °C, 40 V, 1 min.). The polished samples were used for mapping of structure by EBSD. The etched (3s, Vilella-Bain reagent) electropolished samples were used for observation of structure by SEM.

The characterization of microstructure and chemistry of fine precipitates was done at high resolution transmission electron microscope (HTEM) JEOL JEM-2100F with X-Max80 Oxford Instruments EDS detector including also selected area electron diffraction (SEAD). HTEM studies were carried out on thin foils and carbon replicas. Thin foils were prepared from 3 x 0.1 mm thick disc by dimpling (spherical grinding), followed by ion milling. The evaluation of phases from SEAD patterns was realized in software JEMS.

3. RESULTS

The structure of all three experimental samples is shown in Figs.1-3. The size of grains and misorientation of structure was analyzed by EBSD and evaluated by software Channel 5. It was found that martensitic structure of the samples changes very slightly. The average grain size is varied from 1.7 μm to 2.04 μm and 2.15 μm and the misorientation angles of internal interfaces of samples A, B, C is very similar (Fig.4). The analysis of the misorientation angles indicates two main groups of boundaries in martensitic matrix: low angle (below 20°) and high angle (50–60°) boundaries. The misorientation micrograph shows practically very similar typical martensitic microstructure in all samples. There are only very small differences in both misorientation and size of grain, which could denoted decomposition of martensitic structure after annealing. But generally, the main process occurred in structure during short annealing of samples B and C is precipitation.

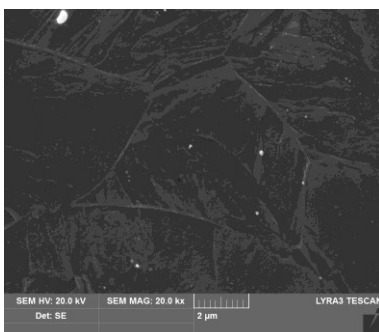


Fig.1 Nb-rich particles in austenitized steel P91, sample A

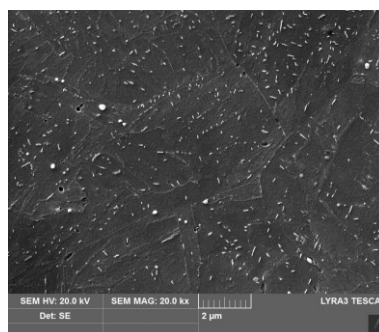


Fig.2 Precipitation of particles after annealing, sample B.

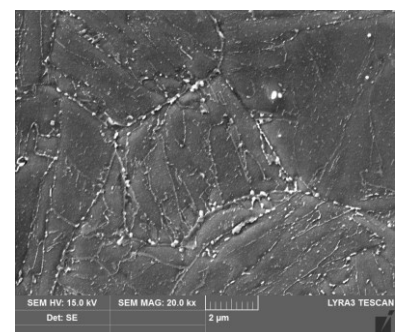


Fig.3 Precipitation of particles after annealing, sample C.

The austenitized structure of sample A contained only round particles (Fig.1). However, the different types of secondary phases was observed in the structure after short annealing of 2 hours at 623 and 823 K. Very fine needle-like particles precipitated mainly in grain interiors in structure of sample B (Fig.2). In contrast with sample C annealed at 823 K, where the structure contained mainly particles precipitated at grain and subgrain boundaries (Fig.3). The needle-like precipitates were not primarily observed in structure of sample C.

The main types of particles were analyzed in carbon replicas by EDS and SAED pattern in HTEM. The main elements identifying type of particles are chromium or niobium, whereas the content of Si, Cu and C in carbon layer is irrelevant. It was found, that the EDS chemical analysis identified particles very well and its result agreed with results by SAED patterns (Fig.5).

The sample A contained only few rounded particles usually identified as Nb-rich MX type particles [6, 12]. These particles had higher content of Nb (~86 wt.%) and V (~9 wt.%) and some of them was identified also as M₂X type particles by SEAD pattern (Fig. 5). These particles were found in structure of all samples.

The Fe (~80 wt.%) and Cr-rich (~11 wt.%) needle-like precipitates were identified by EDS as M₃C type particles (Fig. 6). These similar residual M₃C particles were also found in steel X12CrMoWVNbN10-1-1 [5]. The particles formed in sample C were mainly identified as Cr,Mo,V-rich M₇C₃ and M₂₃C₆ precipitates (Fig.7,8). The carbides M₇C₃ contained about 68 wt.% Cr, 11 wt.% Mo and 3 wt.% V and the carbides M₂₃C₆ about 76 wt.% Cr, 5% wt.% Mo and 1.5 wt.% V. Therefore, the carbide M₂₃C₆ contained roughly half content of Mo and V in comparison with carbide M₇C₃.

The typical locations of precipitates are shown in structure of sample C. The precipitates M₂₃C₆ were located particularly in grain boundaries (GB) of original austenite grains and sparsely also inside subgrains (Fig. 3,9,10). Their typical shape is ellipsoidal with aspect ratio from interval of 2.7 - 3.8. The smaller lath-like particles M₇C₃, precipitated approximately with much higher aspect ratio of about 2 – 12 located primarily in subgrain GBs (Fig. 10). There are obvious also small M₃C (~20 x 2 nm) type particle. Nevertheless, these needle-like precipitates were found especially in sample B and their typical aspect ratio was about 220 nm x 15 nm (Fig. 2). The Nb-rich MX and M₂X particles occurred in structure mainly inside of original austenitic grains.

4. DISCUSSION

The size of grains and GB misorientation of original austenitic grains and subgrains was without significant changes after annealing for 2 h at 673 and 873 K (Fig. 4). Although, the structure is called martensitic, it is practically supersaturated BCC structure and not HCP or BCT martensitic structure and the ratio of cell parameters *c/a* is 1. For example, it has been shown that martensite has a supersaturated BCC structure in the low carbon range up to 0.6 wt.% C in Fe-C

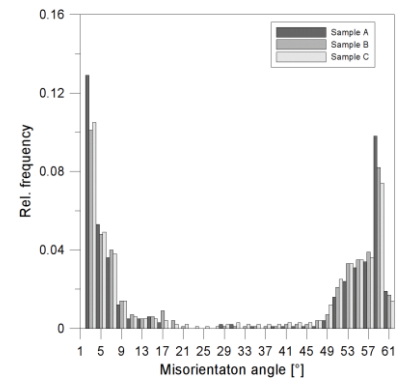


Fig.4 The histogram of misorientation angles of internal interfaces.

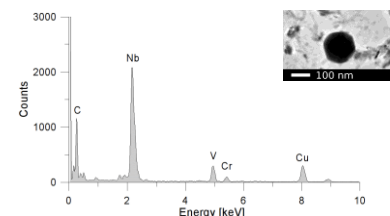


Fig.5 Example of EDS spectrum and SEAD pattern of Nb-rich M₂X particle.

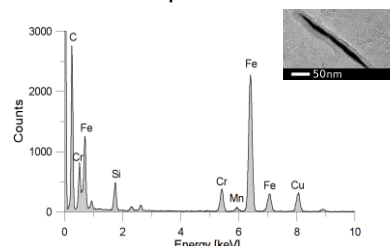


Fig.6 EDS spectrum of extracted M₃C particle.

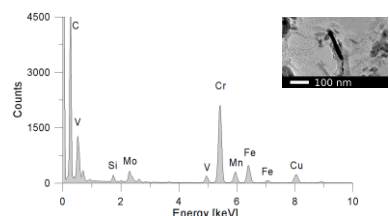


Fig.7 EDS spectrum of extracted M₇C₃ particle.

alloy [6]. It has been reported that below the 0.6 wt.%C only primary martensite is created as BCC iron plus a carbon-rich phase. The constant value of $c/a = 1$ for C concentrations from 0 to 0.6 wt.% was interpreted as evidence for the formation of martensite with the BCC structure, containing a meta-stable C-rich phase (P). The transformation was designated as primary martensite and follows the sequence FCC → HCP and HCP → BCC+P [3]. Generally, this supersaturated system reached the equilibrium primarily by the precipitation of carbides.

The Fe,Cr-rich M_3C precipitated firstly under temperature M_s (sample B). Above this temperature mainly Cr-Mo-V rich carbides M_7C_3 , $M_{23}C_6$ started to form (sample C). But also very thin and small M_3C particles were observed. They are significantly smaller than in structure of sample B. This indicated, that the sequence of carbide precipitation can be similar as in steel X12CrMoWVNbN10-1-1. This process can be summarized as follows: Fe-rich M_3C → Cr – rich M_7C_3 → Cr – rich $M_{23}C_6$ [5]. It was mentioned above, that the M_3C in Cr-Mo containing alloy steels, precipitates from supersaturated ferrite via a paraequilibrium transformation mechanism. This mechanism of precipitation of M_3C in Cr-Mo steel was studied in paper [3]. There was found, that the concentration of the substitutional alloying elements in the cementite near the cementite/matrix interface was not observed as it could be expected by equilibrium thermodynamics. These concentrations were found experimentally to be the same in cementite in both a low carbon and a high carbon alloy which have significantly different equilibrium levels with respect to the solute elements. This fact leads to the conclusion that diffusion of the solutes through the matrix and within the cementite is the rate-controlling step during the early stages of the enrichment process. The interface concentration gradually rise from those dictated by paraequilibrium towards the equilibrium concentrations. This transformation could be controlled rather by the interstitial diffusion of carbon than diffusion of substitutional elements.

In ours previous paper [4], the carbon diffusion was studied in temperature interval 573–1073 K in carbon-supersaturated surface layer of ferrite 9Cr–1Mo steel P91. Extremely low carbon diffusion coefficient D_C (by 3 orders of magnitude lower than equilibrium value $D_{C_{eq}}$) was observed in carburized region. Above the temperature M_s , the values of D_C were close to the values published in the literature for the carbon diffusion coefficient in the carbide phase. Whereas up to temperature M_s , the value of D_C increased and approached the value of $D_{C_{eq}}$. These results correlated very well with precipitation of carbides described at the present paper. Above temperature M_s precipitates mainly Cr-Mo-V-rich M_7C_3 , $M_{23}C_6$ carbides. It can be expected, that the carbon is “trapped” by these substitutional elements Cr,Mo,V that they slowdown the carbon diffusion. Under temperature M_s , precipitate Fe,Cr-rich M_3C carbides, where the content of chromium is slightly higher than average content in steel P91, Fe,Cr rich M_3C carbides precipitated. In contrast to temperatures above temperature M_s , here the carbon is influenced only slightly by precipitation of M_3C , therefore, it can able to diffuse through BCC quite freely. It is the reason, why the value of D_C increased and approaches the value $D_{C_{eq}}$ reported for carbon in chemically equilibrated matrix.

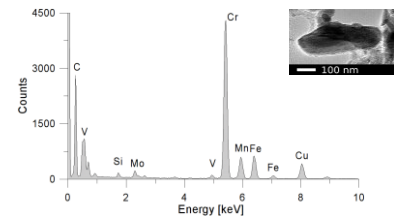


Fig.8 EDS spectrum of extracted $M_{23}C_6$ particle.

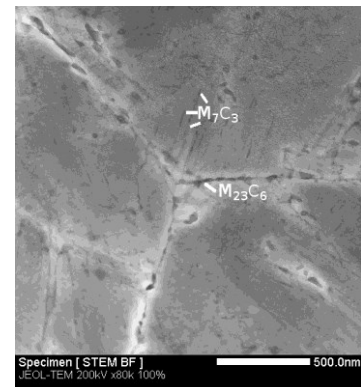


Fig. 9 Original austenite grains of sample C, examples of main types of precipitates.

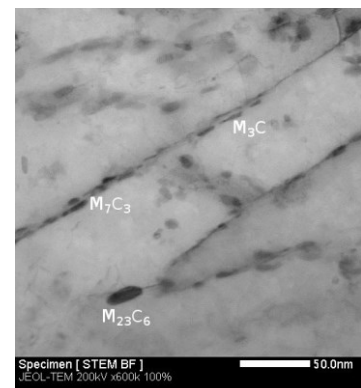


Fig. 10 Martensite laths in sample C, examples of main types of precipitates.

CONCLUSION

In the present work, the structure and precipitation of carbides after annealing for 2 h at temperatures 673 K and 873 K was studied. It was found that:

- 1) Up to temperature M_s , mainly Fe,Cr-rich M_3C carbides precipitates, while above M_s the mainly precipitation of Cr-Mo-V-rich M_7C_3 , $M_{23}C_6$ carbides starts.
- 2) The carbon diffusion is strongly influenced by precipitation of Cr-Mo-V-rich M_7C_3 , $M_{23}C_6$ carbides. This process results in very slow carbon diffusion above temperature M_s in supersaturated matrix.
- 3) The sequence of carbides precipitation seems to be same as in steel X12CrMoWVNbN10-1-1: Fe-rich $M_3C \rightarrow$ Cr – rich $M_7C_3 \rightarrow$ Cr – rich $M_{23}C_6$.

ACKNOWLEDGEMENTS

This work was supported by project CEITEC - Central European Institute of Technology, project number CZ.1.05/1.1.00/02.0068 and by financial support by the Ministry of Education, Youth and Sport of the Czech Republic throughout the project No. CZ.1.07/2.3.00/20.0214 (Human Resources Developments in the research of physical and material properties of emerging, newly developed and applied engineering materials).

REFERENCES

- [1] SANTELLA M.L., SWINDERMAN R.W., REED R.W., TANZOSH J.M. Martensite transformation, microsegregation, and creep strength of 9 Cr-1 Mo-V steel weld metal, Oak Ridge National Laboratory: Oak Ridge, 2001, <http://web.ornl.gov/~webworks/cppri/y2001/pres/113751.pdf> .
- [2] SKLENICKA V., KUCHAROVÁ V., SVOBODA M., KROUPA A., CMAKAL J. Creep behavior and microstructural changes of advanced creep resistant steels after long-term isothermal ageing. Mater. Sci. Forum, Vol. 654-656, 2010, pp. 504-507.
- [3] SHERBY O.D., WADSWORTH J., LESUER R.D. Revisiting the Structure of Martensite in Iron-Carbon Steels. Materials transaction, Vol. 49, No. 9, 2008, pp. 2016-2027.
- [4] THOMSON R.C., MILLER M.K. Carbide precipitation in martensite during the early stages of tempering Cr- and Mo-containing low alloy steels. Acta Materialia, Vol. 46, No. 6, 1998, pp. 2203-2213.
- [5] CERMAK J., KRAL L. Effect of carbon-supersaturation upon the carbon diffusion in 9Cr-1Mo ferrite steel. Materials Letters, Vol. 116, 2014, pp. 402-404.
- [6] TAO X., GU J., HAN L. Characterization of precipitates in X12CrMoWVNbN10-1-1 steel during heat treatment. Journal of Nuclear Materials, Vol. 452, No. 1-3, 2014, pp. 557-564.
- [7] SHERBY O.D., WADSWORTH J., SYN C.K. The c/a Ratio in Quenched Fe-C and Fe-N Steels - A Heuristic Story. Materials Science Forum, Vol. 539-543, 2007, pp. 215-222.